Jordan Journal of Pharmaceutical Sciences, Volume 16, No. 4, 2023

Fabrication of Interpenetrating Polymer Network-Based Hydrogel for Colon-Targeted Release of Nateglinide

Daxaben Kothiya[1], Subhash Vaghani[2]*

[1] Manager, Powerhouse Pharmacy, Dallas, USA
[2] CMD, Harvin Labs, Ankleshwar, India.

ABSTRACT

Nateglinide is an anti-diabetic agent that experiences modest first-pass metabolism and poor aqueous solubility. This paper explores the preparation, characterization, and evaluation of interpenetrating polymer network composite hydrogels of chitosan and poly(meth(methacrylic)) acid as a potential carrier for the drug. Interpenetrating polymer network composite hydrogels of chitosan and poly(meth(methacrylic) acid incorporating nateglinide were prepared using N,N'-methylene bisacrylamide and glutaraldehyde as cross-linkers. The polymerization of chitosan, entrapment of the drug, and its interaction in prepared hydrogels were checked by FTIR spectroscopy, DSC, and powder XRD studies. The hydrogels were evaluated for their swelling behavior and in vitro drug release. The morphology of the hydrogels before and after dissolution was studied using SEM. The hydrogels showed a 93.29 ± 4.65% yield and 91.28 ± 2.22% drug loading. The hydrogels exhibited pH-sensitive swelling behavior. The in vitro release profile confirmed that the drug release depended on the swelling of hydrogels and showed a biphasic release pattern. Chitosan-poly(meth(methacrylic)) acid interpenetrating polymer network hydrogel, with its biodegradable nature and pH-sensitive release of nateglinide, is an attractive option to be further explored for targeted controlled drug delivery formulations for the drug.

Keywords: Chitosan-Poly(meth(methacrylic)) Acid hydrogel; Interpenetrating Polymer Network; Nateglinide; Biodegradable; pH-Sensitive.

INTRODUCTION

Nateglinide (NAT) is used for the treatment of type 2 diabetes. This blood-glucose-lowering drug belongs to the meglitinide class[1]. NAT has been classified to belong to Class II per the Biopharmaceutical Classification System[2] as it has good intestinal permeability but inadequate water solubility of 0.061 mg/mL[3]. In addition to selectively blocking beta-cells of the pancreas, it has a short half-life of 1.5 to 2.5 hours[4]. Rapid intestinal absorption is observed with NAT. In the physiological intestinal environment, where pH is approximately 6.5, the compound is predominantly ionized due to its pKa value of 3.1[5]. Over a dose range of 62 - 240 mg, the drug displays linear pharmacokinetics, with no dose-dependent time to peak concentration[6]. CYP2C9 and CYP3A4 are the primary cytochrome P450 enzymes involved in its biotransformation in the liver [7]. After oral administration of 120 mg of the drug 10 minutes before a meal, peak plasma concentrations of 10.08 g/mL are reached in approximately 0.5 - 1.0 hours[8]. The short half-life and variable bioavailability of this drug may be due to its poor solubility in water, both of which could be improved by sustaining its release over time.

Interpenetrating polymer networks (IPN) have been around since 1914, when Aylsworth invented the first one[9]. IPN refers to a network composed of at least two polymers,

****Corresponding author: Subhash Vaghani***
subhashvaghani@gmail.com
Received: 3/1/2023 Accepted: 7/8/2023.
DOI: https://doi.org/10.35516/jjps.v16i4.775

one synthesized in the presence of the other. A physical crosslinking network is formed when polymer chains in the second system entwine with polymer chains in the first system [10]. Since each polymer retains its unique properties, synergistic improvements in characteristics such as strength or toughness are observed. Additionally, it's important to note that IPNs differ from polymer blends in that they exhibit swelling behavior without dissolution in solvents, and they effectively suppress creep and flow.

As a consequence of exhibiting superior performance compared to conventional individual polymers, Interpenetrating Polymer Networks (IPN) have witnessed a surge in applications. Their advanced properties have garnered significant attention in the pharmaceutical industry, especially in the realm of drug delivery. With the ability to create nontoxic, biocompatible, and biodegradable polymer networks, IPNs are gaining prominence for delivering bioactive molecules, particularly in the context of controlled and targeted drug delivery. The versatility of IPNs is evident through the multitude of molecules produced via this approach, all aimed at enhancing targeting and bioavailability [11–14]. Over the years, formulators have focused fabricated these IPNs into various dosage forms [15–23]. They have also made them smarter by making them respond to stimuli such as magnets [24], temperature [25], pH [26], ions [27], electrons [28], and light [29].

A hydrogel is a polymeric material capable of holding large amounts of water in its three-dimensional network due to its hydrophilic nature[30]. Despite its ability to swell and retain moisture, a hydrogel does not dissolve in water. The hydrophilic functional groups attached to the polymer backbone contribute to its water-absorbing properties, while crosslinking between network chains imparts resistance to dissolution[31]. Hydrogels derived from natural polymers, such as chitosan, have garnered significant attention due to their biocompatibility and the ease of preparing newer derivatives. However, unmodified chitosan faces challenges such as low mechanical strength and limited control over the release of entrapped molecules, stemming from its hydrophilic nature and excellent solubility in an acidic medium. Therefore, using modified chitosan hydrogels for the controlled delivery of bioactive molecules is beneficial [32,33]. One such modification is the formation of Interpenetrating Polymer Networks. Chitosan-Poly(meth(methacrylic)) Acid (C-PMMA) hydrogels are an example of IPN exhibiting good mechanical strength and pH-sensitive swelling behavior [34]. These hydrogels have been explored for the controlled release of drugs like amoxicillin [35], meloxicam [35], and metronidazole [36], to name a few. The current paper investigates the synthesis, characterization, and evaluation of this IPN as a potential carrier for the slow release of NAT.

RESULTS

Characterization of chitosan

Chitosan's molecular weight and N-deacetylation percentage were measured as 3.5×10^5 Da and 84.6%, respectively.

High performance liquid chromatography analysis

It was observed that NAT's retention time was 5.3 min, with a single, sharp peak being obtained. The method was linear in the range of 2.5 to 20 µg/mL. According to the calibration curve, the slope was 80440, and the intercept was -43720. The correlation coefficient was 0.9984.

Synthesis of chitosan-poly(meth(methacrylic)) acid IPN hydrogel, yield calculation and drug loading

C-PMMA IPN was synthesized through a solution co-polymerization/crosslinking reaction, employing potassium persulfate (KPS) as a redox initiator to initiate polymerization. The results, including yield and drug loading for various samples, have been tabulated in Table 1.

Table 1: Yields and drug loading obtained for different formulations of hydrogels

Formulation	Yield (%) n = 3 ± SD	Drug loading (%) n = 3 ± SD
K1	93.29 ± 4.65	91.28 ± 2.22
K2	95.38 ± 2.63	89.95 ± 2.91
K3	94.13 ± 3.46	92.88 ± 3.02
K4	92.58 ± 2.11	93.47 ± 2.78

Swelling studies

IPNs' swelling properties depend heavily on their gel structure, crosslinking density, and surrounding medium composition[37]. The percentage swelling index for the hydrogels under different pH conditions is depicted in **Figure 1**.

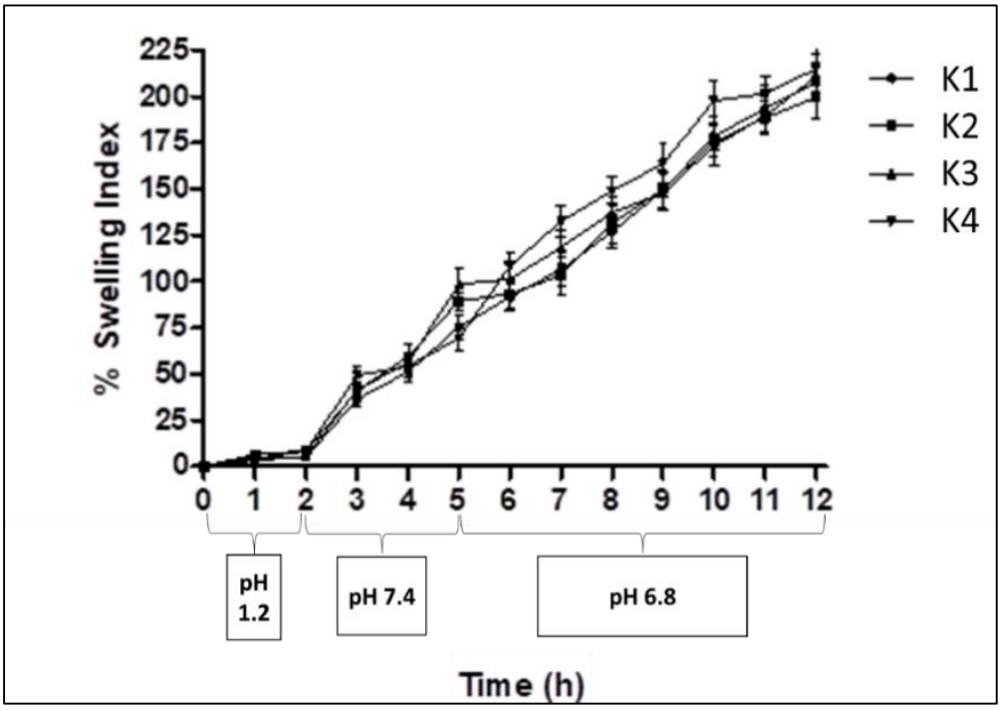

Figure 1. % Swelling Index for C-PMMA IPN hydrogels containing NAT (n = 3)

In vitro drug release studies and release kinetics

Figure 2 shows the cumulative release of NAT from C-PMMA IPN hydrogels at different pH conditions. In all four hydrogels, only K1 released NAT almost entirely after 12 h; therefore, it was considered an optimized formulation.

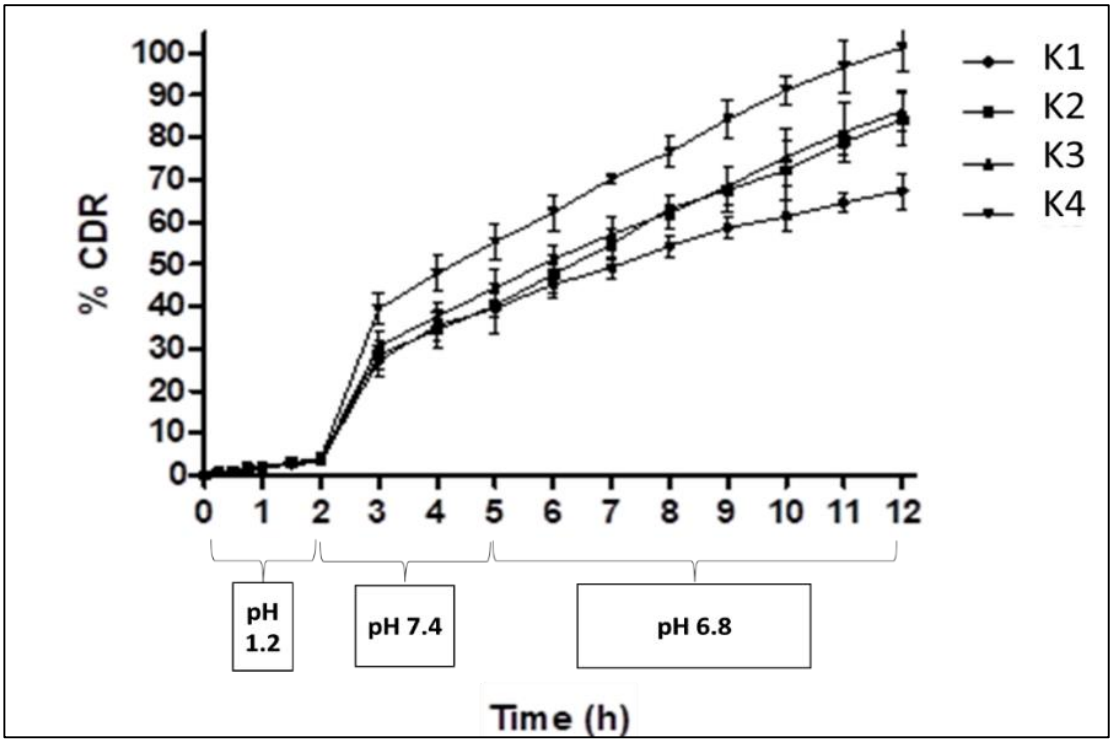

Figure 2. % Cumulative Drug Release (CDR) under different pH conditions for NAT from C-PMMA IPN hydrogel

The release of the drug followed zero-order kinetics (R^2 = 0.9965) for the middle three hours (from hours two to five) when the dissolution media used was phosphate buffer pH 7.4. It displayed Korsmeyer Peppas non-Fickian diffusion (diffusion coupled with erosion) kinetics with n > 0.5 at the higher pH of 6.8 (R^2 = 0.9932, n = 0.6406). According to our studies, the pH-dependent C-PMMA IPN hydrogel system does assist in the controlled release of NAT in the colon, which could contribute to improved oral bioavailability of the drug.

FTIR spectroscopic study

The FTIR spectra of chitosan, C-PMMA IPN hydrogels and NAT are given in **Figure 3**.

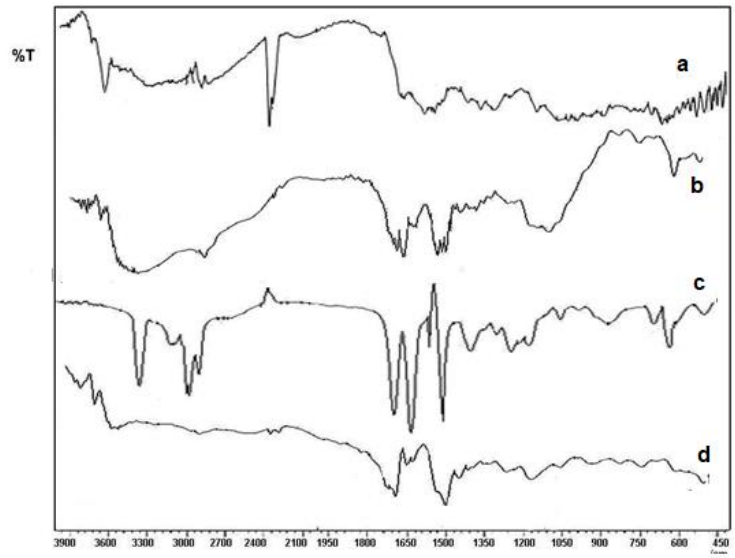

Figure 3: FTIR spectra of (a) Chitosan, (b) blank C-PMMA IPN hydrogels, (c) NAT, and (d) NAT-loaded C-PMMA IPN hydrogels

Differential Scanning Calorimetry study

DSC analysis was performed to characterize the thermal behavior of chitosan, C-PMMA IPN, and NAT in the hydrogel formulation. The endotherms obtained are shown in Figure 4.

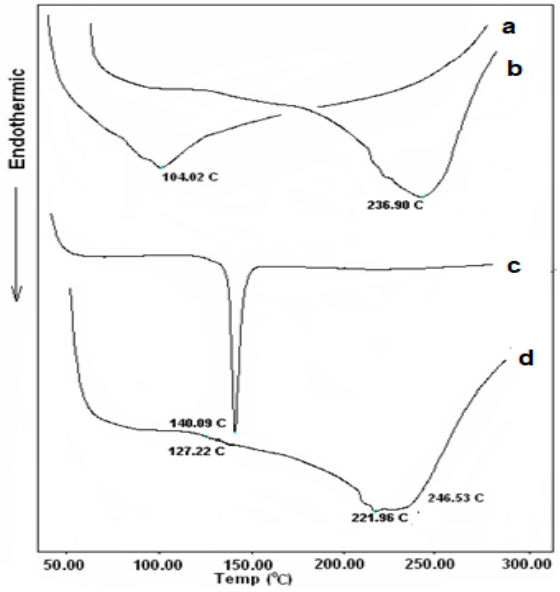

Figure 4: DSC thermogram of (a) Chitosan, (b) Blank C-PMMA IPN, (c) NAT, and (d) NAT-loaded C-PMMA IPN formulation

Powder X-Ray diffractometry study

The X-ray diffractograms of chitosan, blank C-PMMA IPN, NAT, and NAT-loaded C-PMMA IPN are shown in Figure 5.

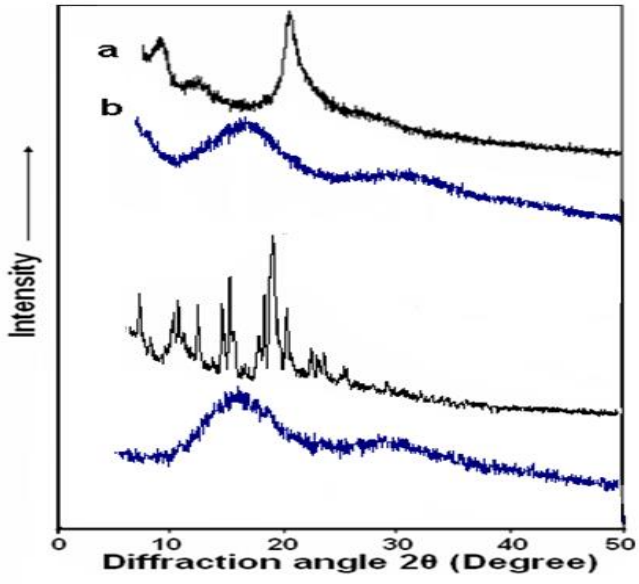

Figure 5: X-ray diffractogram of (a) Chitosan, (b) Blank C-PMMA IPN, (c) NAT, and (d) NAT-loaded C-PMMA IPN formulation

Scanning electron microscopy study

A surface morphology study was conducted on an optimized hydrogel containing NAT before and after dissolution. The surface morphology showed a translucent non-porous membrane (Fig. 6a). Following dissolution, the surface morphology revealed the presence of open channel-like structures (Fig. 6b).

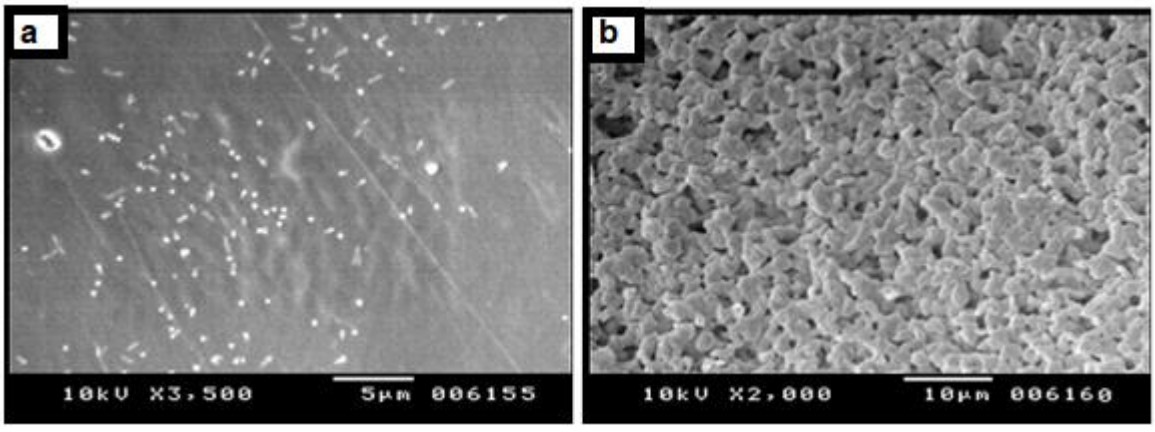

Figure 6: SEM of C-PMMA IPN containing NAT (a) Before dissolution and (b) After the dissolution

Determination of unreacted glutaraldehyde and methacrylic acid

The gas chromatography study conducted to quantify glutaraldehyde levels in the formulations revealed that only 4.1 ppm of the crosslinker remains. Furthermore, the unreacted monomer accounted for 1.54 mg. These two values confirmed that the proportion of unreacted material was small enough not to affect the toxicity or stability of the formulation.

DISCUSSION

Synthesis of chitosan-poly(meth(methacrylic)) acid IPN hydrogel, yield calculation and drug loading

Aqueous solutions of KPS decompose into sulphate ion Aqueous solutions of KPS decompose into sulfate ion radicals, which further react with water to produce hydroxyl radicals. In this scenario, chitosan acts as a weak reducing agent, forming chitosan radicals in response to these hydroxyl radicals, leading to further polymerization propagation[38]. NH_3^+ groups in chitosan and COO^- groups in poly(meth(methacrylic)) acid can interact electrostatically to form polyelectrolytes[39]. As a result of the presence of a solvent, heat is dissipated. After preparing the hydrogels, they were washed with distilled water to remove the monomer, oligomer, crosslinking agent, initiator, soluble and extractable polymer, and other impurities.

Swelling studies

The intrinsic pKa of chitosan is 6.5, below which NH_2 groups are ionized, i.e., they are in the $–NH_3^+$ form. At pH levels above 4.5, carboxylic groups in methacrylic acid become ionized [40]. Due to the combination of anionic and cationic groups, the prepared hydrogels were amphiphilic. Additionally, anions crosslink with chitosan. In acidic conditions (pH = 1.2), acid groups are not ionized, and swelling is mainly controlled by protonated amino groups ($–NH_3^+$) attached to the C2 carbon of the chitosan [41]. Within these hydrogels, poly(meth(methacrylic)) acid might help protonate amines from chitosan, causing electrostatic repulsion between chains of polymers [42]. Due to the polymer's charges, chitosan chains are electrostatically repelled from each other, and a higher osmotic pressure is created inside the gel. Gel swelling balances the difference in osmotic pressure between the network's internal and external solutions [41]. However, the swelling was not observed in the present case due to high crosslink densities due to glutaraldehyde. Poly(meth(methacrylic)) acid ionizes above pH 4.5, resulting in higher swelling. Chitosan amino groups were ionized at pH 6.8, and ionic bonds dissociated. This led to the increased swelling ratio of the hydrogel due to the electrostatic repulsion of COO^- ions from poly(meth(methacrylic)) acid. A similar phenomenon was seen in the ileocecal phase of the study [41]. A hydrogel's maximum swelling level is determined by the balance between contractile and repulsive forces within the network. There is a possibility of the complex dissolving if there is a high level of swelling. If we maximize the number of electrostatic interactions between two oppositely charged polymers, the grade of network complexation will be maximized. As a result, the network will become more stable, reducing swelling/eroding behavior in hydrogels. Due to its tighter structure, the network will be able to control the release of drugs [43]. The C-PMMA IPN hydrogels were made by crosslinking chitosan with glutaraldehyde; therefore, the amino groups present were meagre. Furthermore, the degree of swelling is inversely proportional to the crosslinking; therefore, the degree of swelling would decrease at all pH values compared to plain chitosan hydrogels.

In vitro drug release studies and release kinetics

C-PMMA IPN are hydrophilic that can absorb water and swell in an aqueous environment. When the IPN come into contact with a surrounding medium, such as a physiological solution, they absorb water and increase in size. The swelling of the IPN creates pores and channels within the polymer matrix [12]. As the C-PMMA IPN swell, the drug molecules start to diffuse out of the IPN in response to a concentration gradient. The rate of diffusion

is influenced by factors such as the molecular weight and size of the drug molecules, the degree of cross-linking of the polymer, and the nature of the surrounding medium [44]. NAT is released biphasically in response to pH changes in the hydrogel. The polymer used is a pH-responsive one which is soluble at pH 6 and above. Thus, the polymer did not swell or solubilize at pH 1.2 which mimicked the acidic conditions of the stomach [45]. C-PMMA IPN hydrogels are amphiphilic since they contain both anionic and cationic groups. Chitosan's protonated amino groups were mainly responsible for controlling the swelling of these hydrogels; under acidic conditions, this effect was negligible. As a result, drug release in the first two hours in SGF was also insignificant. However, as pH increased, swelling increased, resulting in an increase in drug release from the hydrogel [46]. In addition to diffusion, the drug release from C-PMMA IPN can also be affected by polymer degradation. PMMA is known to undergo hydrolysis under certain conditions, resulting in the breakdown of polymer chains. The degradation of the polymer can lead to the release of encapsulated drug molecules. The rate of polymer degradation depends on factors such as pH, temperature, and the presence of enzymes or other catalysts [47]. Overall, the drug release from C-PMMA IPN involves a combination of swelling, diffusion, and polymer degradation. These factors collectively contribute to the pH-dependent controlled and sustained release of drugs from the polymer matrix, allowing for precise modulation of drug delivery kinetics [48].

FTIR spectroscopic study

FTIR spectrum of chitosan revealed a broad absorption band in the 3500 and 3100 cm^{-1} range, centered at 3400 cm^{-1}, due to O–H stretching vibration, N-H extension vibration and the intermolecular H-bonds of the polysaccharide moieties (Fig. 3a). Axial stretching of C–H–bonds were observed corresponding to a band at 2881 cm^{-1}. A peak at 1676 cm^{-1} is attributed to the axial stretching of C=O bonds of the acetamide group which indicated that the sample was not fully acetylated. A band at 1557 cm^{-1} owing to the angular deformation of the N–H bonds of the amino group was observed. A band at 1370 cm^{-1} due to the symmetrical angular deformation of CH_3 and the amide III band at 1320 cm^{-1} were also noted. The band in the range 1156-898 cm^{-1} corresponding to the polysaccharide skeleton, including the vibrations of the glycoside bonds, C–O and C–O–C stretching was observed [49,50].

In C-PMMA IPN hydrogels (Fig. 3b), an additional peak around 1720 cm^{-1} was observed which represented carboxylate ion. Negatively charged carboxylate ion and positively charged NH_3^+ co-existed in C-PMMA IPN hydrogels [51]. New peaks at 1530-1540 cm^{-1} were found in the blank IR spectra of C-PMMA IPN hydrogels probably due to the ionic interaction between chitosan and the acids. Glutaraldehyde was used as cross-linking agent for chitosan, hence an additional peak at 1680 cm^{-1} was observed indicating the formation of Schiff's base as a result of the reaction between the carbonyl group of glutaraldehyde and amine group of chitosan chains ensuring the proper formation of the IPNs [52,53].

The FTIR spectrum of NAT (Fig. 3c) revealed peaks at 3184.25 cm^{-1} due to NH stretching; at 3064.68 cm^{-1} and 2948.96 cm^{-1} attributed to alkyl and phenyl stretching, respectively; 2655.68 cm^{-1} due to N^+ stretching; 1685.68 cm^{-1} due to C=O stretching; 1525.59 cm^{-1} and 1385.23 cm^{-1} due to symmetric and asymmetric stretching of NO_2 group; 1470.5 cm^{-1} and 1385.23 cm^{-1} due to bending of geminal methyl group and at 781.12 cm^{-1} and 703.97 cm^{-1} due to out of plane bending of 5 and 3 adjacent hydrogen of the aromatic ring [54]. All these peaks were exhibited in the FTIR spectrum of optimized C-PMMA IPN hydrogel containing NAT also (Fig. 3d), which confirmed the presence of the drug in the hydrogel without any significant alteration of the functional group owing to reaction with other ingredients of the hydrogel.

Differential Scanning Calorimetry study

At 104.02 °C, pure chitosan displayed a broad melting endotherm (Fig. 4a). IPN C-PMMA (Fig. 4b) exhibited melting endotherms at 236.99 °C. Amidation between

chitosan and poly(meth(methacrylic)) acid may explain the higher glass transition temperature (Tg). The carboxylate groups and carboxyl groups in the C-PMMA IPN react when heated to 200 °C, producing amide bonds between the ammonium groups and non-protonated amino groups of chitosan [34]. NAT exhibited a sharp endotherm at 140.90 °C (Fig. 4c), which matches its melting point [55]. In C-PMMA IPN, NAT did not show sharp melting endotherms (Fig 4d), indicating either an amorphous form of the drug or a solid solution.

Powder X-Ray diffractometry study

Chitosan's XRD pattern presented the most intense diffraction intensity in the broad peak between 17 and 23 degrees, which reflected the semicrystalline nature of the material (Fig. 5a), as reported by the literature [56]. According to Figure 5b, there is no sharp crystalline peak in the diffraction pattern of the blank C-PMMA IPN, which indicates its amorphous nature. NAT's diffraction pattern (Fig. 5c) showed characteristic peaks at 8.16°, 11.54°, 13.14°, 15.22°, 15.98°, 19.76° and 21.06°, indicating its crystalline nature [57]. NAT-loaded C-PMMA IPN formulations are devoid of all sharp peaks, as seen in the diffractogram (Fig. 5d). As a result, it was determined that the drug was amorphous in the final formulation.

Scanning electron microscopy study

The open channel-like structures could be due to the ionization of carboxyl groups and dissociation of ionic crosslinks between chitosan and poly(meth(methacrylic)) acid, which is consistent with swelling results.

EXPERIMENTAL SECTION

General Experimental

Methacrylic acid was sourced from Sigma Aldrich, USA. Chitosan was donated by Central Marine Fisheries Research Institute (Cochin, India). NAT was obtained as a gift sample from Zydus Research Centre, Ahmedabad (India). N,N-methylene-bis-acrylamide and Potassium persulfate were purchased from S.D. Fine Chem. Ltd., India and Ranbaxy Fine Chemicals Ltd., India, respectively. All other chemicals and reagents such as acetonitrile, methanol, phosphoric acid used were of analytical grades and used as received.

Characterization of chitosan

In a solvent containing 0.1 M acetic acid and 0.2 M NaCl maintained at 25 °C, the average molecular weight of chitosan was determined by Mark-Houwink viscometry [49].

The degree of N-deacetylation was determined by FTIR using the following relationship:

$$\%N - deacetylation = 100\left[1 - \left(\frac{A_{1655}}{A_{3398}}\right)\left(\frac{1}{1.33}\right)\right] \quad (1)$$

In this case, A corresponds to the absorbance at the given wave number, whereas 1676 and 3400 cm^{-1} correspond to amide and chitosan primary amino groups, respectively. In the case of fully N-acetylated chitosan, factor 1.33 represents the A_{1676}/A_{3400} [58].

High performance liquid chromatography analysis

In this study, High Performance Liquid Chromatography (HPLC) measurements were conducted using Shimadzu's LC 2010 AHT system, equipped with a UV/ Visible detector. We analyzed the samples on a Kromasil C18 column (250 x 4.6 mm ID, 5 m pore size) equipped with an auto integrator. In the mobile phase, 0.067 M monobasic potassium phosphate, acetonitrile and methanol in a 60:30:10 % v/v ratio. The flow rate was 1.0 mL per minute at 50 °C for 15 minutes at a pressure of 1500 PSI. A wavelength of 210 nm was used to detect NAT with a retention time of 5.3 minutes [59]. This study used a calibration curve based on concentrations ranging from 2.5 µg/mL to 20 µg/mL to evaluate all samples (with 20 µL injection volume).

Synthesis of chitosan-poly(meth(methacrylic)) acid IPN hydrogel, yield calculation and drug loading

C-PMMA IPN hydrogels incorporating NAT were prepared using N, N'-methylene bisacrylamide (MBA) and glutaraldehyde as crosslinkers in the presence of redox initiator, KPS. To prepare a methacrylic acid monomer solution, 2.8 g of methacrylic acid were dissolved in 0.1 M

acetic acid (5 mL). Next, we carried out the polymerization reaction in flasks by dissolving 1 g of chitosan in 2% acetic acid (40 mL), followed by adding a monomer solution of methacrylic acid. NAT was added to this solution. To initiate the reaction, KPS (108 mg) was added, followed by MBA (4 mg) and glutaraldehyde (0.15 mL). The polymerization flask was placed in a thermostatic bath at an elevated temperature of 120 °C for one hour. After allowing the mass to cool to room temperature, it was filtered and washed several times with distilled water to remove unreacted chemical contaminants [60]. The formulae for the trials for the preparations of IPN are given in **Table 2**.

Table 2: Formulae for C-PMMA IPN hydrogels

Ingredients	**Formulations**			
	K1	**K2**	**K3**	**K4**
Chitosan (g)	1.0	1.0	1.0	1.0
Methacrylic acid (g)	2.8	2.8	2.8	2.8
KPS (mg)	108	108	108	108
MBA (mg)	4.0	4.0	4.0	4.0
Glutaraldehyde 25% (mL)	0.15	0.15	0.15	0.15
NAT (g)	0.5	1.0	1.5	2.0

The yields of the resultant hydrogels were calculated using the formula:

$$\% \text{ Yield} = \left(\frac{A}{B}\right) \times 100 \quad (2)$$

Where A is the actual weight of the hydrogel and B is the theoretical weight of the hydrogel.

Crushed hydrogel samples containing 10 mg of NAT were used to determine drug loading. After weighing and transferring the hydrogel samples to a 10 mL volumetric flask, the volume was filled with methanol. Keeping the solution aside allowed the insoluble matter to settle. Next, a 10 mL volumetric flask was filled with 5 ml of supernatant clear liquid, which was then diluted with mobile phase to volume and mixed. Using the predefined HPLC method, ten µl of the solution was assayed. The concentration of NAT was calculated, and drug loading was determined using the following formula:

$$\% \text{ Drug Loading } = \left(\frac{X}{Y}\right) \times 100 \quad (3)$$

X is the actual concentration of NAT in the hydrogel, and Y is the theoretical concentration of NAT in the hydrogel.

Swelling studies

Hydrogels were soaked in buffer solutions, and incubated at 37°C under 150 rpm, and their swelling behavior was measured. In the first step, dry hydrogels were immersed in 0.1 M HCl solution at pH 1.2 for two hours (gastric phase). After that, the hydrogels were transferred to a sodium phosphate buffer solution at pH 7.4 and were allowed to stand for three hours (small intestine phase). In the final step, they were transferred to a sodium phosphate buffer solution at a pH of 6.8 for seven hours (colonic phase) [61,62]. Samples were removed from the swelling medium at certain intervals and blotted with filter paper to remove excess moisture. To calculate the percentage of swelling, SI, at each time, we used the following expression [41] :

$$\%SI = \left[\frac{W_t - W_0}{W_0}\right] \times 100 \quad (4)$$

W_t and W_0 are the sample weights at time t and in the dry state, respectively.

In vitro drug release studies and release kinetics

In vitro dissolution studies of NAT from hydrogels were conducted using a USP XXIV dissolution rate test apparatus (type II, model TDT-08 L, Electrolab, Mumbai, India) fitted with a paddle (100 rev/min) at 37 °C. Dissolution was conducted in 250 mL simulated gastric fluid (SGF, pH 1.2) for two hours, in 900 mL phosphate buffer solution (PBS, pH 7.4) for three hours, and then in

900 mL PBS (pH 6.8) for 12 hours. A sample equivalent to 90 mg of NAT was taken for in vitro drug release studies [63,64]. An aliquot of five mL was withdrawn at predetermined times, filtered through a 0.45-µm membrane filter, diluted, and analyzed using the previously described HPLC method. Using the calibration curve, the % CDR was calculated.

Based on the results of in vitro release studies, various kinetic equations were fitted to determine the likely mechanism of the release of drugs from prepared hydrogels. The kinetic models used in this study were zero order, first order, Higuchi, and Korsmeyer-Peppas models. For each model, rate constants were calculated.

Fourier-transformed infrared (FTIR) spectroscopic study

By analyzing the FTIR spectra recorded for chitosan, NAT, C-PMMA IPN, and optimized formulation, we evaluated the changes in polymer structure after forming hydrogels, crosslinking and the drug-polymer interactions. An FTIR spectrophotometer (FTIR-8400 S, Shimadzu, Japan) was used to record the spectra using KBr pellets in a scanning range of 400-4000 cm^{-1} at a resolution of 2 cm^{-1}.

Differential scanning calorimetry (DSC) study

NAT, C-PMMA IPN, and optimized formulation, were scanned using an automatic thermal analyzer (DSC 60, Shimadzu, Japan) equipped with time domain spectroscopy tread line software. The experiments were conducted using sealed aluminium-lead pans. At a scanning rate of 10 °C/min, the samples were heated from 50-300 °C.

Powder X-Ray diffractometry (PXRD) study

The powder X-ray diffraction study was carried out to characterize chitosan, NAT, C-PMMA IPN and the optimized formulation. X-rays were generated using a Philips X'Pert 3040/60 in Almelo, Netherlands, capable of emitting CuKα radiation (λ=1.54178Å). Data was collected in continuous scan mode at 0.01° steps at 2θ in the scanning range of 5–50°.

Scanning electron microscopy (SEM) study

To examine the surface morphology of the optimized formulation, scanning electron microscopy was used before and after dissolution. A dried film was first mounted on a stub using double-sided adhesive tape. Then, a scanning electron microscope (JEOL, JSM-5600 LV, Japan) was used to observe the films after they had been coated with gold to determine their surface characteristics.

Determination of unreacted glutaraldehyde and methacrylic acid

Gas chromatography was used to determine the amount of unreacted glutaraldehyde. To prepare the standard solution, glutaraldehyde (100 mg) was diluted to 10 mL with N, N-di-methyl pyrrolidone (NMP). First, a 0.2 mL sample was diluted to 10 mL with NMP, after which 0.1 mL was withdrawn and further diluted to 10 mL with NMP. A volume of 5 mL of the resulting standard solution was injected into a gas chromatograph (2014, Shimadzu). One gram of blank C-PMMA IPN was dissolved in five mL NMP and injected into the headspace of a gas chromatograph. The amount of unreacted glutaraldehyde was obtained using the following equation:

$$\frac{AUC_{sample}}{AUC_{std}} \times \frac{0.1}{10} \times \frac{0.2}{10} \times \frac{0.1}{10} \times \frac{5}{1} \times 10^6 \quad (7)$$

The titrimetric analysis determined the amount of unreacted methacrylic acid[65]. A blank formulation containing C-PMMA was immersed in 100 mL of distilled water for 48 hours to dissolve the unreacted monomer. Afterward, it was filtered and diluted with distilled water to a total volume of 100 mL. One drop of phenolphthalein was added to this solution, and it was titrated against a 0.001 N sodium hydroxide solution. Each milliliter of NaOH was equated with 0.08609 mg of methacrylic acid.

CONCLUSION

NAT was entrapped in the IPN hydrogel by crosslinking chitosan with poly(meth(methacrylic)) acid without significant changes in its chemical composition, as evident from the characterization of the hydrogel. In vitro drug release studies and swelling studies of hydrogels

show a direct correlation between swelling and drug release from the hydrogel. The NAT hydrogel delivers its drug biphasically from the hydrogel, with minimal drug release under acidic conditions in the stomach, followed by continuous release under alkaline conditions in the colon. Consequently, this hydrogel would be ideal for releasing NAT into the colon after bypassing the stomach. As NAT is delivered to the colon specifically, the drug's metabolism would be reduced to a great extent, which is the leading cause of the low bioavailability of NAT. Accordingly, we conclude that the C-PMMA IPN hydrogel may be an effective carrier for NAT to increase its oral bioavailability. Because hydrogels are nontoxic and biodegradable, they represent a promising drug delivery system as a cost-effective, straightforward dosage form.

ACKNOWLEDGMENTS: None.
CONFLICT OF INTEREST: None.
FINANCIAL SUPPORT: N. A.
ETHICS STATEMENT: None.

REFERENCES

1. Tentolouris N, Voulgari C, Katsilambros N. A review of nateglinide in the management of patients with type 2 diabetes. *Vasc Health Risk Manag*. 2007; 3(6): 797-807.
2. Wairkar S, Gaud R, Jadhav N. Enhanced dissolution and bioavailability of Nateglinide by microenvironmental pH-regulated ternary solid dispersion: in-vitro and in-vivo evaluation. *J Pharm Pharmacol*. 2017; 69(9): 1099-1109. https://doi.org/10.1111/jphp.12756
3. Sahoo RK, Biswas N, Guha A, Sahoo N, Kuotsu K. Development and in vitro/in vivo evaluation of controlled release provesicles of a nateglinide-maltodextrin complex. *Acta Pharm Sin B*. 2014; 4(5): 408-416. https://doi.org/10.1016/j.apsb.2014.08.001
4. Vinod M, Jitendra N, Komal P, Rahul C, Gokul K. Enhancement of Solubility with Formulation & in-vitro Evaluation of Oral Nateglinide Compacts by Liquisolid Technique. *Advances in Diabetes and Metabolism*. 2013; 1(3): 57-64. https://doi.org/10.13189/adm.2013.010302
5. Terada T, Sawada K, Saito H, Hashimoto Y, Inui K. Inhibitory effect of novel oral hypoglycemic agent nateglinide (AY4166) on peptide transporters PEPT1 and PEPT2. *Eur J Pharmacol*. 2000; 392(1-2): 11-17. https://doi.org/10.1016/s0014-2999(00)00119-9
6. Keilson L, Mather S, Walter YH, Subramanian S, McLeod JF. Synergistic effects of nateglinide and meal administration on insulin secretion in patients with type 2 diabetes mellitus. *J Clin Endocrinol Metab*. 2000; 85(3): 1081-1086. https://doi.org/10.1210/jcem.85.3.6446
7. Guardado-Mendoza R, Prioletta A, Jiménez-Ceja LM, Sosale A, Folli F. The role of nateglinide and repaglinide, derivatives of meglitinide, in the treatment of type 2 diabetes mellitus. *Arch Med Sci*. 2013; 9(5): 936-943. https://doi.org/10.5114/aoms.2013.34991
8. Devineni D, Walter YH, Smith HT, Lee JS, Prasad P, McLeod JF. Pharmacokinetics of Nateglinide in Renally Impaired Diabetic Patients. *The Journal of Clinical Pharmacology*. 2003; 43(2): 163-170. https://doi.org/10.1177/0091270002239825
9. Aylsworth JW. Plastic composition. Published online September 22, 1914. Accessed February 8, 2022. https: //patents.google.com/patent/US1111284A/en
10. Lohani A, Singh G, Bhattacharya SS, Verma A. Interpenetrating Polymer Networks as Innovative Drug Delivery Systems. *Journal of Drug Delivery*. 2014; 2014: 1-11. https://doi.org/10.1155/2014/583612

11. Kulkarni RV, Sreedhar V, Mutalik S, Setty CM, Sa B. Interpenetrating network hydrogel membranes of sodium alginate and poly(vinyl alcohol) for controlled release of prazosin hydrochloride through skin. *International Journal of Biological Macromolecules*. 2010; 47(4): 520-527. https://doi.org/10.1016/j.ijbiomac.2010.07.009
12. Xu Q, Huang W, Jiang L, Lei Z, Li X, Deng H. KGM and PMAA based pH-sensitive interpenetrating polymer network hydrogel for controlled drug release. *Carbohydrate Polymers*. 2013; 97(2): 565-570. https://doi.org/10.1016/j.carbpol.2013.05.007
13. Boppana R, Kulkarni RV, Mutalik SS, Setty CM, Sa B. Interpenetrating network hydrogel beads of carboxymethylcellulose and egg albumin for controlled release of lipid lowering drug. *Journal of Microencapsulation*. 2010; 27(4): 337-344. https://doi.org/10.3109/02652040903191842
14. Malakar J, Nayak AK, Pal D. Development of cloxacillin loaded multiple-unit alginate-based floating system by emulsion–gelation method. *International Journal of Biological Macromolecules*. 2012; 50(1): 138-147. https://doi.org/10.1016/j.ijbiomac.2011.10.001
15. Kumar P, Pillay V, Choonara YE. Macroporous chitosan/methoxypoly (ethylene glycol) based cryosponges with unique morphology for tissue engineering applications. *Sci Rep*. 2021; 11(1): 3104. https://doi.org/10.1038/s41598-021-82484-x
16. Kondolot Solak E, Er A. pH-sensitive interpenetrating polymer network microspheres of poly(vinyl alcohol) and carboxymethyl cellulose for controlled release of the nonsteroidal anti-inflammatory drug ketorolac tromethamine. *Artificial Cells, Nanomedicine, and Biotechnology*. 2016; 44(3): 817-824. https://doi.org/10.3109/21691401.2014.982805
17. Nita LE, Chiriac AP, Rusu AG, et al. Stimuli Responsive Scaffolds Based on Carboxymethyl Starch and Poly(2-Dimethylaminoethyl Methacrylate) for Anti-Inflammatory Drug Delivery. *Macromol Biosci*. 2020; 20(4): e1900412. https://doi.org/10.1002/mabi.201900412
18. Boschetti PJ, Toro DJ, Ontiveros A, Pelliccioni O, Sabino MA. Lattice Boltzmann method simulations of swelling of cuboid-shaped IPN hydrogel tablets with experimental validation. *Heat Mass Transfer*. Published online October 10, 2021. https://doi.org/10.1007/s00231-021-03132-8
19. Dai Z, Yang X, Wu F, et al. Living fabrication of functional semi-interpenetrating polymeric materials. *Nat Commun*. 2021; 12(1): 3422. https://doi.org/10.1038/s41467-021-23812-7
20. Hasan MdM, Chisty AH, Rahman MM, Khan MN. Bioprotein Based IPN Nanoparticles as Potential Vehicles for Anticancer Drug Delivery: Fabrication Technology. In: Jana S, Jana S, eds. *Interpenetrating Polymer Network: Biomedical Applications*. Springer; 2020: 183-203. https://doi.org/10.1007/978-981-15-0283-5_7
21. Abou El-Ela RM, Freag MS, Elkhodairy KA, Elzoghby AO. Interpenetrating Polymer Network (IPN) Nanoparticles for Drug Delivery Applications. In: Jana S, Jana S, eds. *Interpenetrating Polymer Network: Biomedical Applications*. Springer; 2020: 25-54. https://doi.org/10.1007/978-981-15-0283-5_2
22. Kadri R, Elkhoury K, Ben Messaoud G, et al. Physicochemical Interactions in Nanofunctionalized Alginate/GelMA IPN Hydrogels. *Nanomaterials*. 2021; 11(9): 2256. https://doi.org/10.3390/nano11092256
23. Li S, Shao C, Miao Z, Lu P. Development of leftover rice/gelatin interpenetrating polymer network films for food packaging. *Green Processing and Synthesis*. 2021; 10(1): 37-48. https://doi.org/10.1515/gps-2021-0004
24. Mohammad Gholiha H, Ehsani M, Saeidi A, Ghadami A, Alizadeh N. Magnetic dual-responsive semi-IPN nanogels based on chitosan/PNVCL and study on BSA release behavior. *Prog Biomater*. 2021; 10(3): 173-183. https://doi.org/10.1007/s40204-021-00161-8
25. Qin Z, Zhang R, Xu Y, Cao Y, Xiao L. A one-pot synthesis of thermosensitive PNIPAAM interpenetration polymer networks(IPN) hydrogels. *JCIS Open*. 2021; 1: 100002. https://doi.org/10.1016/j.jciso.2021.100002

26. Lim LS, Rosli NA, Ahmad I, Mat Lazim A, Mohd Amin MCI. Synthesis and Swelling Behavior of pH-Sensitive Semi-IPN Superabsorbent Hydrogels Based on Poly(acrylic acid) Reinforced with Cellulose Nanocrystals. *Nanomaterials (Basel)*. 2017; 7(11): E399. https://doi.org/10.3390/nano7110399
27. Dragan ES, Cocarta AI. Smart Macroporous IPN Hydrogels Responsive to pH, Temperature, and Ionic Strength: Synthesis, Characterization, and Evaluation of Controlled Release of Drugs. *ACS Appl Mater Interfaces*. 2016; 8(19): 12018-12030. https://doi.org/10.1021/acsami.6b02264
28. Sarmad S, Yenici G, Gürkan K, Keçeli G, Gürdağ G. Electric field responsive chitosan–poly(N,N-dimethyl acrylamide) semi-IPN gel films and their dielectric, thermal and swelling characterization. *Smart Mater Struct*. 2013; 22(5): 055010. https://doi.org/10.1088/0964-1726/22/5/055010
29. Zhou L, Ma T, Li T, Ma X, Yin J, Jiang X. Dynamic Interpenetrating Polymer Network (IPN) Strategy for Multiresponsive Hierarchical Pattern of Reversible Wrinkle. *ACS Appl Mater Interfaces*. 2019; 11(17): 15977-15985. https://doi.org/10.1021/acsami.8b22216
30. Almasri R, Swed A, Alali H. Preparation and Characterization of Hydrogel Beads for Controlled Release of Amoxicillin. *Jordan Journal of Pharmaceutical Sciences*. 2022; 15(4): 523-535. https://doi.org/10.35516/jjps.v15i4.675
31. Ahmed EM. Hydrogel: Preparation, characterization, and applications: A review. *Journal of Advanced Research*. 2015; 6(2): 105-121. https://doi.org/10.1016/j.jare.2013.07.006
32. Giri TK, Thakur A, Alexander A, Ajazuddin, Badwaik H, Tripathi DK. Modified chitosan hydrogels as drug delivery and tissue engineering systems: present status and applications. *Acta Pharmaceutica Sinica B*. 2012; 2(5): 439-449. https://doi.org/10.1016/j.apsb.2012.07.004
33. Abudayah AAF. Implication of Nanotechnology for Pulmonary Delivery of Docetaxel. *Jordan Journal of Pharmaceutical Sciences*. 2023; 16(2): 470-470. https://doi.org/10.35516/jjps.v16i2.1527
34. Lee JW, Kim SY, Kim SS, Lee YM, Lee KH, Kim SJ. Synthesis and characteristics of interpenetrating polymer network hydrogel composed of chitosan and poly(acrylic acid). *Journal of Applied Polymer Science*. 1999; 73(1): 113-120. https://doi.org/10.1002/(SICI)1097- 4628(19990705)73: 1<113: : AID-APP13>3.0.CO; 2-D
35. Wang Y, Wang J, Yuan Z, et al. Chitosan cross-linked poly(acrylic acid) hydrogels: Drug release control and mechanism. *Colloids and Surfaces B: Biointerfaces*. 2017; 152: 252-259. https://doi.org/10.1016/j.colsurfb.2017.01.008
36. Yadav KH, Satish CS, Shivakumar HG. Preparation and evaluation of chitosan-poly (acrylic acid) hydrogels as stomach specific delivery for amoxicillin and metronidazole. *Indian Journal of Pharmaceutical Sciences*. 2007; 69(1): 91. https://doi.org/10.4103/0250-474X.32115
37. Milosavljević NB, Milašinović NZ, Popović IG, Filipović JM, Kalagasidis Krušić MT. Preparation and characterization of pH-sensitive hydrogels based on chitosan, itaconic acid and methacrylic acid: pH-sensitive hydrogels based on Ch, IA and MAA. *Polym Int*. 2011; 60(3): 443-452. https://doi.org/10.1002/pi.2967
38. Yazdani-Pedram M, Retuert J, Quijada R. Hydrogels based on modified chitosan, 1. Synthesis and swelling behavior of poly(acrylic acid) grafted chitosan. *Macromolecular Chemistry and Physics*. 2000; 201(9): 923-930. https://doi.org/10.1002/1521-3935(20000601)201: 9<923: : AID-MACP923>3.0.CO; 2-W

39. Wang H, Li W, Lu Y, Wang Z. Studies on chitosan and poly(acrylic acid) interpolymer complex. I. Preparation, structure, pH-sensitivity, and salt sensitivity of complex-forming poly(acrylic acid): Chitosan semi-interpenetrating polymer network. *Journal of Applied Polymer Science*. 1997; 65(8): 1445-1450. https://doi.org/10.1002/(SICI)1097-4628(19970822)65: 8<1445::AID-APP1>3.0.CO; 2-G
40. Fujiwara M, Grubbs RH, Baldeschwieler JD. Characterization of pH-Dependent Poly(acrylic Acid) Complexation with Phospholipid Vesicles. *Journal of Colloid and Interface Science*. 1997; 185(1): 210-216. https://doi.org/10.1006/jcis.1996.4608
41. Tavakol M, Vasheghani-Farahani E, Dolatabadi-Farahani T, Hashemi-Najafabadi S. Sulfasalazine release from alginate-N,O-carboxymethyl chitosan gel beads coated by chitosan. *Carbohydrate Polymers*. 2009; 77(2): 326-330. https://doi.org/10.1016/j.carbpol.2009.01.005
42. Torre P. Release of amoxicillin from polyionic complexes of chitosan and poly(acrylic acid). study of polymer/polymer and polymer/drug interactions within the network structure. *Biomaterials*. 2003; 24(8): 1499-1506. https://doi.org/10.1016/S0142-9612(02)00512-4
43. Silva CL, Pereira JC, Ramalho A, Pais AACC, Sousa JJS. Films based on chitosan polyelectrolyte complexes for skin drug delivery: Development and characterization. *Journal of Membrane Science*. 2008; 320(1-2): 268-279. https://doi.org/10.1016/j.memsci.2008.04.011
44. Helal SH, Abdel-Aziz HMM, El-Zayat MM, Hasaneen MNA. Preparation, characterization and properties of three different nanomaterials either alone or loaded with nystatin or fluconazole antifungals. *Sci Rep*. 2022; 12(1): 22110. https://doi.org/10.1038/s41598-022-26523-1
45. Brady J, Dürig T, Lee PI, Li JX. Chapter 7 - Polymer Properties and Characterization. In: Qiu Y, Chen Y, Zhang GGZ, Yu L, Mantri RV, eds. *Developing Solid Oral Dosage Forms (Second Edition)*. Academic Press; 2017: 181-223. https://doi.org/10.1016/B978-0-12-802447-8.00007-8
46. Hhr C, K C, Ja LP, et al. Design and Optimization of a Nanoparticulate Pore Former as a Multifunctional Coating Excipient for pH Transition-Independent Controlled Release of Weakly Basic Drugs for Oral Drug Delivery. *Pharmaceutics*. 2023; 15(2). https://doi.org/10.3390/pharmaceutics15020547
47. Tian Y, Lei M. Polydopamine-Based Composite Nanoparticles with Redox-Labile Polymer Shells for Controlled Drug Release and Enhanced Chemo-Photothermal Therapy. *Nanoscale Res Lett*. 2019; 14(1): 186. https://doi.org/10.1186/s11671-019-3027-6
48. Duarte Junior AP, Tavares EJM, Alves TVG, et al. Chitosan nanoparticles as a modified diclofenac drug release system. *J Nanopart Res*. 2017; 19(8): 274. https://doi.org/10.1007/s11051-017-3968-6
49. El-Sherbiny IM. Enhanced pH-responsive carrier system based on alginate and chemically modified carboxymethyl chitosan for oral delivery of protein drugs: Preparation and in-vitro assessment. *Carbohydrate Polymers*. 2010; 80(4): 1125-1136. https://doi.org/10.1016/j.carbpol.2010.01.034
50. de Abreu FR, Campana-Filho SP. Characteristics and properties of carboxymethylchitosan. *Carbohydrate Polymers*. 2009; 75(2): 214-221. https://doi.org/10.1016/j.carbpol.2008.06.009
51. Nam S. Pervaporation and properties of chitosan-poly(acrylic acid) complex membranes. *Journal of Membrane Science*. 1997; 135(2): 161-171. https://doi.org/10.1016/S0376-7388(97)00144-0
52. Risbud MV, Hardikar AA, Bhat SV, Bhonde RR. pH-sensitive freeze-dried chitosan-polyvinyl pyrrolidone hydrogels as controlled release system for antibiotic delivery. *J Control Release*. 2000; 68(1): 23-30. https://doi.org/10.1016/s0168-3659(00)00208-x
53. Banerjee T, Mitra S, Kumar Singh A, Kumar Sharma R, Maitra A. Preparation, characterization and biodistribution of ultrafine chitosan nanoparticles. *International Journal of Pharmaceutics*. 2002; 243(1): 93-105. https://doi.org/10.1016/S0378-5173(02)00267-3

54. Bruni G, Berbenni V, Milanese C, et al. Thermodynamic relationships between nateglinide polymorphs. *J Pharm Biomed Anal*. 2009; 50(5): 764-770. https://doi.org/10.1016/j.jpba.2009.06.017
55. Bruni G, Berbenni V, Milanese C, et al. Determination of the nateglinide polymorphic purity through DSC. *J Pharm Biomed Anal*. 2011; 54(5): 1196-1199. https://doi.org/10.1016/j.jpba.2010.12.003
56. Neira-Carrillo A, Yazdani-Pedram M, Retuert J, Diaz-Dosque M, Gallois S, Arias JL. Selective crystallization of calcium salts by poly(acrylate)-grafted chitosan. *J Colloid Interface Sci*. 2005; 286(1): 134-141. https://doi.org/10.1016/j.jcis.2004.12.046
57. Goyal P, Rani D, Chadha R. Exploring structural aspects of nateglinide polymorphs using powder X-ray diffraction. *International Journal of Pharmacy and Pharmaceutical Sciences*. Published online October 2, 2017: 119-127. https://doi.org/10.22159/ijpps.2017v9i10.20795
58. El-Sherbiny IM. Synthesis, characterization and metal uptake capacity of a new carboxymethyl chitosan derivative. *European Polymer Journal*. 2009; 45(1): 199-210. https://doi.org/10.1016/j.eurpolymj.2008.10.042
59. Bauer S, Störmer E, Kirchheiner J, Michael C, Brockmöller J, Roots I. Rapid and simple method for the analysis of nateglinide in human plasma using HPLC analysis with UV detection. *J Pharm Biomed Anal*. 2003; 31(3): 551-555. https://doi.org/10.1016/s0731-7085(02)00680-5
60. Neira-Carrillo A, Yazdani-Pedram M, Retuert J, Diaz-Dosque M, Gallois S, Arias JL. Selective crystallization of calcium salts by poly(acrylate)-grafted chitosan. *J Colloid Interface Sci*. 2005; 286(1): 134-141. https://doi.org/10.1016/j.jcis.2004.12.046
61. Raj BS, Shanthi, Nair RS, Samraj PI, Vidya. Formulation and Evaluation of Coated Microspheres for Colon Targeting. *J App Pharm Sci*. 2013; 3(8): S68-S74. https://doi.org/10.7324/JAPS.2013.38.S11
62. Ren Y, Jiang L, Yang S, et al. Design and preparation of a novel colon-targeted tablet of hydrocortisone. *Braz J Pharm Sci*. 2016; 52: 239-250. https://doi.org/10.1590/S1984-82502016000200002
63. Jin L, Ding YC, Zhang Y, Xu XQ, Cao Q. A novel pH-enzyme-dependent mesalamine colon-specific delivery system. *Drug Des Devel Ther*. 2016; 10: 2021-2028. https://doi.org/10.2147/DDDT.S107283
64. Maity S, Kundu A, Karmakar S, Sa B. In Vitro and In Vivo Correlation of Colon-Targeted Compression-Coated Tablets. *Journal of Pharmaceutics*. 2016; 2016: e5742967. https://doi.org/10.1155/2016/5742967
65. Alfrey Jr. T, Pinner SH. Preparation and titration of amphoteric polyelectrolytes. *Journal of Polymer Science*. 1957; 23(104): 533-547. https://doi.org/10.1002/pol.1957.1202310402

تصنيع هلام قائم على الشبكة البوليمرية المتداخلة لإطلاق ناتيغلينيد المستهدف للقولون

داكسابين كوثيا[1]، سوبهاش فاغاني[2]*

[1] مدير صيدلية باورهاوس، دالاس، الولايات المتحدة الأمريكية.

[2] CMD، مختبرات هارفين، أنكليشوار، الهند.

ملخص

ناتيغلينيد هو عامل مضاد لمرض السكري الذي يعاني من هضم متواضع في المرور الأول وذوبان مائي ضعيف. تستكشف الورقة الحالية إعدادًا وتوصيفًا وتقييمًا لشبكات البوليمر المتداخلة المركبة للهيدروجيلات المركبة من الكيتوزان وحمض البولي (الميثاكريليك) كحامل محتمل للدواء. تم تحضير شبكات البوليمر المتداخلة المركبة للهيدروجيلات من الكيتوزان وحمض البولي (الميثاكريليك) التي تتضمن ناتيغلينيد باستخدام N,N'- ميثيلين بيساكريلاميد وغلوتارالديهيد كعوامل ربط. تم فحص البلمرة من الشيتوزان ، فخ الدواء وتفاعله في الهلاميات المائية المعدة عن طريق التحليل الطيفي FTIR، DSC ومسحوق XRD الدراسات للمسح الضوئي للمسح الضوئي للمسح الضوئي. تم تقييم الهيدروجيلات لسلوكها في الانتفاخ وإطلاق الدواء في الكشف الخارجي. درست مورفولوجيا الهيدروجيلات قبل وبعد الانحلال باستخدام. SEM أظهرت الهيدروجيلات نسبة عائد تبلغ 93.29 ± 4.65 % ونسبة تحميل الدواء تبلغ 91.28 ± 2.22 %. أظهرت الهيدروجيلات سلوك انتفاخ حساس لقيم ال .pH أكد ملف الإطلاق في المختبر أن إطلاق الدواء يعتمد على انتفاخ الهيدروجيلات وأظهر نمط إطلاق ثنائي الطور. هلام الكيتوزان–حمض البولي (الميثاكريليك) المتداخل للشبكة البوليمرية مع طبيعته القابلة للتحلل والإطلاق الحساس لقيم ال pH لناتيغلينيد خيار جذاب يجب استكشافه بشكل أوسع لصياغات توصيل الدواء المستهدفة والمحكومة للدواء.

الكلمات الدالة: هلام الكيتوزان–حمض البولي (الميثاكريليك) ؛ شبكة البوليمر المتداخلة ؛ ناتيجلينيد ؛ قابلة للتحلل ؛ حساس لقيم ال .pH

* ***المؤلف المراسل: سوبهاش فاغاني***

subhashvaghani@gmail.com

تاريخ استلام البحث: 2023/1/3 وتاريخ قبوله للنشر: 2023/8/7.